

tion of synapses elsewhere in the nervous system of *Drosophila* and probably in mammals as well.

## REFERENCES AND NOTES

- C. S. Goodman and C. J. Shatz, *Cell* **72**, 77 (1993); C. S. Goodman, *Annu. Rev. Neurosci.*, in press.
- M. Bate and K. Broadie, *Neuron* **15**, 513 (1995).
- K. Broadie *et al.*, *Dev. Suppl.* (1993), p. 227.
- A detailed description of the methods is available from the authors or at <http://fruitfly.berkeley.edu> (C. C. Koppczynski, T. Serano, G. R. Rubin, C. S. Goodman, in preparation).
- LBL appears to be expressed by all motoneurons whose axons exit in the two major motor nerves (the intersegmental and segmental nerves) and innervate somatic body wall muscles; LBL is probably not expressed by motor axons that exit other nerves and innervate visceral and respiratory muscles.
- The small amount of *lbl* expression in peripheral sensory neurons begins at stage 14 and disappears by stage early 17.
- A 189-base pair (bp) Pst fragment from the *p3B6* cDNA was cloned into the Pst site of pQE31 (Qiagen) to fuse a six-histidine affinity tag onto the NH<sub>2</sub>-terminus of LBL amino acids 85 to 148. This region corresponds to the last 8 amino acids of TM3 and the first 55 amino acids of the large extracellular loop. The fusion protein was expressed with QIAexpress (Qiagen) and injected into mice, and antiserum was tested histologically on embryos. The specificity of the antiserum for LBL was confirmed by its failure to stain *lbl<sup>Y13</sup>* embryos.
- A 1.2-kb insert in cDNA clone *p3B6.6* was subcloned as six smaller fragments into Bluescript SK+ (Stratagene). Double-stranded template DNA was sequenced on both strands by means of the Auto-read sequencing kit (Pharmacia) and ALF automated sequencer (Pharmacia).
- DNA and protein databases were searched with the program BLAST [S. F. Altschul *et al.*, *J. Mol. Biol.* **215**, 403 (1990)].
- V. Horejsi and C. Vlcek, *FEBS Lett.* **288**, 1 (1991); M. L. Gil *et al.*, *J. Immunol.* **148**, 2826 (1992); T. Imai *et al.*, *ibid.* **149**, 2879 (1992); M. G. Tomlinson, A. F. Williams, M. D. Wright, *Eur. J. Immunol.* **23**, 136 (1993).
- CD37 and CD53, two tetraspanins most closely related to LBL, share 29% amino acid identity with one another but only 19% and 16% amino acid identity, respectively, with LBL. Sequence similarity among tetraspanins is highest in and between TM2 and TM3; in this region, CD37 and CD53 share 39% amino acid identity, whereas LBL shares 27% amino acid identity with CD37 and 25% identity with CD53.
- The *lbl* gene was mapped to polytene band 42F1 by *in situ* hybridization. Two P-element stocks containing insertions in the 42F1 region, S64 and Y13, were obtained from the Berkeley *Drosophila* Genome Center. The genomic DNA flanking each of these P-elements was isolated by the inverse polymerase chain reaction [B. Dalby, A. J. Pereira, L. S. B. Goldstein, *Genetics* **139**, 757 (1995)] and sequenced. Both P-elements were inserted in a 5' untranslated exon of the *lbl* gene. In line *P(w+)*S64 the P-element was inserted 225 bp upstream, whereas *P(w+)*Y13 was inserted 151 bp upstream of the start of translation. Each stock was backcrossed for 10 generations against the parental *w<sup>1118</sup>* background to remove any modifiers of the mutant phenotype.
- The 1D4 mAb recognizes Fasciclin II, a marker for motor axons, growth cones, and terminal arbors [D. Van Vactor *et al.*, *Cell* **73**, 1137 (1993)].
- Staging of embryos was done with attention to head involution, CNS condensation, gut morphology, and 1D4 mAb staining (13) [J. A. Campos-Ortega and V. Hartenstein, *The Embryonic Development of Drosophila melanogaster* (Springer-Verlag, Berlin, 1985)].
- There appears to be a reciprocal relation between RP3 innervation and ectopic sprouting onto muscles 7 and 6 in *lbl* mutant embryos. At stage late 16, the RP3 terminal arbor was absent in 50% of hemisegments ( $n = 132$ ); 41% ( $n = 109$ ) displayed ectopic TN arborizations. At stage early 17, the RP3 terminal arbor was missing in 22% of hemisegments ( $n = 137$ ) and ectopic TN arborizations were seen in 49% ( $n = 136$ ). In contrast, in control (*w<sup>1118</sup>*) embryos, the RP3 terminal arbor was absent in only 12% of stage late 16 hemisegments ( $n = 128$ ) and in only 2% of stage early 17 hemisegments ( $n = 118$ ). Ectopic TN arborizations were observed in 11% of stage late 16 control embryos ( $n = 114$ ) and in 3% of stage early 17 control embryos ( $n = 127$ ).
- This tendency of the TN to sprout onto muscles 6 and 7 in the absence of a functional RP3 synapse has been observed previously [H. Keshishian *et al.*, *J. Neurobiol.* **24**, 757 (1993); J. Jarecki and H. Keshishian, *J. Neurosci.* **15**, 8177 (1995)].
- First-instar larvae were selected 0 to 5 hours after hatching and dissected. Synaptic boutons were visualized with a polyclonal antibody to synaptotagmin [J. T. Littleton *et al.*, *Development* **118**, 1077 (1993)]. Boutons were counted in segments A2 to A5. The mean numbers of boutons ( $\pm$ SD) were  $14.5 \pm 3.5$  for the control (Canton S) ( $n = 37$ ) and  $14.3 \pm 3.4$  for the *lbl* mutant ( $n = 67$ ).
- J. B. Thomas, M. J. Bastiani, M. Bate, C. S. Goodman, *Nature* **310**, 203 (1984); H. Sink and P. M. Whittington, *Development* **112**, 307 (1991).
- T. Imai, M. Kakizaki, M. Nishimura, O. Yoshie, *J. Immunol.* **155**, 1229 (1995); G. M. Bell, W. E. Seaman, E. C. Neimi, J. B. Imbolden, *J. Exp. Med.* **175**, 527 (1992); S. Kitani, E. Berentstein, S. Mergenhausen, P. Tempst, R. P. Siraganian, *J. Biol. Chem.* **266**, 1903 (1991); J. J. Roberts, S. E. Rodgers, J. Drury, L. K. Ashman, J. V. Lloyd, *Brit. J. Haematol.* **89**, 853 (1995); E. Rubinstein, F. Le Naour, M. Billard, M. Prenant, C. Boucheix, *Eur. J. Immunol.* **24**, 3005 (1994); F. Berditchevski, G. Bazzoni, M. E. Hemler, *J. Biol. Chem.* **270**, 17784 (1995).
- S. Lebel-Binay, C. Lagaudriere, D. Fradelizi, H. Conjeaud, *J. Immunol.* **155**, 101 (1995); A. M. Rasmussen, H. K. Blomhoff, T. Stokke, V. Horejsi, E. B. Smeland, *ibid.* **153**, 4997 (1994).
- L. Bosca and P. A. Lazo, *J. Exp. Med.* **179**, 1119 (1994); S. Lebel-Binay, C. Lagaudriere, D. Fradelizi, H. Conjeaud, *J. Leukocyte Biol.* **57**, 956 (1995).
- E. S. Anton, M. Hadjiargyrou, P. H. Patterson, W. D. Matthew, *J. Neurosci.* **15**, 584 (1995).
- A. Masellis-Smith and A. R. Shaw, *J. Immunol.* **152**, 2768 (1994).
- J.-T. Dong *et al.*, *Science* **268**, 884 (1995); S. Ikeyama, M. Koyama, M. Yamaoko, R. Sasada, M. Miyake, *J. Exp. Med.* **177**, 1231 (1993); Z. Si and P. Hershey, *Int. J. Cancer* **54**, 37 (1993).
- S. Tole and P. H. Patterson, *Dev. Dyn.* **197**, 94 (1993); Z. Kaprielian, C. Kyung-Ok, M. Hadjiargyrou, P. H. Patterson, *J. Neurosci.* **15**, 562 (1995); M. Hadjiargyrou and P. H. Patterson, *ibid.*, p. 574.
- B. J. Classon *et al.*, *J. Exp. Med.* **169**, 1497 (1989); M. Amiot, *J. Immunol.* **145**, 4322 (1990); M. J. Metzelaar *et al.*, *J. Biol. Chem.* **266**, 3239 (1991); H. W. Gaugitsch *et al.*, *Eur. J. Immunol.* **21**, 377 (1991); N. Emi *et al.*, *Immunogenetics* **37**, 193 (1993); S. Szala *et al.*, *Proc. Natl. Acad. Sci. U.S.A.* **87**, 6833 (1990); K. M. Davern, M. D. Wright, V. R. Herrmann, G. F. Mitchell, *Mol. Biochem. Parasitol.* **48**, 67 (1991); S. Fitter, T. A. Tetaz, M. C. Berndt, L. K. Ashman, *Blood* **86**, 1348 (1995).
- We thank the Berkeley *Drosophila* Genome Center for providing mapped P-elements and J. P. Forjanic for suggesting the name *late bloomer*. C.C.K. was supported as a Jane Coffin Childs Postdoctoral Fellow and a Howard Hughes Medical Institute Postdoctoral Associate, G.W.D. is an American Cancer Society Postdoctoral Fellow, and C.S.G. is an Investigator with HHMI.

27 October 1995; accepted 29 January 1996

## Replay of Neuronal Firing Sequences in Rat Hippocampus During Sleep Following Spatial Experience

William E. Skaggs and Bruce L. McNaughton

The correlated activity of rat hippocampal pyramidal cells during sleep reflects the activity of those cells during earlier spatial exploration. Now the patterns of activity during sleep have also been found to reflect the order in which the cells fired during spatial exploration. This relation was reliably stronger for sleep after the behavioral session than before it; thus, the activity during sleep reflects changes produced by experience. This memory for temporal order of neuronal firing could be produced by an interaction between the temporal integration properties of long-term potentiation and the phase shifting of spike activity with respect to the hippocampal theta rhythm.

Several lines of circumstantial evidence point to a role for the hippocampus in memory, including numerous reports of amnesia or learning deficits after hippocampal damage (1) and of the presence in several parts of the hippocampus of a robust and long-lasting form of Hebbian synaptic modification known as long-term potentiation (2). Much of the data can be accounted for by a theory postulating that the hippocampus is the heart of a system capable of storing memory traces on the basis of a single, brief experience, after which these

traces are "consolidated" gradually into more permanent storage in the neocortex (3-5). A memory system of this sort would, however, be seriously lacking if it were incapable of encoding information about the order in which events occurred.

Recent studies indicate that hippocampal unit activity during sleep reflects the activity patterns that occurred during the experience that preceded the sleep interval. Pyramidal cells in the CA3 and CA1 regions of the rat hippocampus have long been known to fire in a spatially specific manner in a variety of behavioral paradigms, with each cell firing when the rat is in a particular area of the environment (6):

Arizona Research Laboratories, Division of Neural Systems, Memory, and Aging, University of Arizona, Tucson, AZ 85724, USA.

Pavlidis and Winson (7) found that when a rat spends an extended period of time inside the spatial firing field of a hippocampal pyramidal cell, the firing rate of that cell is increased during an immediately following period of slow-wave sleep (SWS). More recently, Wilson and McNaughton (8), using data recorded in parallel from groups of 50 to 100 hippocampal units, found that pairs of cells with overlapping place fields in an environment showed enhanced correlations during SWS following a period of food-seeking behavior in the environment. Because much of the spike activity in the hippocampus during SWS occurs during "sharp waves" (9) (100- to 200-ms bursts of activity that appear to be generated inside the CA3 region), these results suggest that the hippocampal synaptic matrix encodes information about the patterns of unit activity generated by place-related firing during experience in an environment. Given that the activity patterns during sleep contain information about which groups of hippocampal cells fired together, it is natural to wonder whether they also contain information about the temporal order in which the cells fired. We demonstrate here, using ensemble recording methods similar to those of Wilson and McNaughton (8), that temporal order information is indeed preserved during sleep, and a possible physiological mechanism is outlined.

Hippocampal unit activity was recorded from six male Fisher 344 rats by an array of 12 independently movable four-channel "tetrodes," each of which can pick up distinguishable action potentials from 5 to 20 pyramidal cells if the tetrode is positioned with the electrode tips near the center of the CA1 cell body layer (10). Unit activity was recorded during sleep and also as the rats ran for food reward on one of two apparatuses. The first was an elevated wooden track in the shape of a triangle (Fig. 1A), with each side 75 cm long and 8 cm wide; the second was a similar wooden track, 7 cm wide, in the shape of an 87 cm by 36 cm rectangle. Both apparatuses were placed on a table in the center of a cue-controlled recording area, with numerous salient visual cues scattered around the periphery. The task of the rats was merely to traverse the track repeatedly in the same direction, stopping at two (rectangle) or three (triangle) locations to eat a small food reward (11). For each pair of CA1 pyramidal cells in a data set, a measure of temporal ordering was calculated on the basis of their cross-correlation histogram. The temporal bias  $B_{ij}$  for cells  $i$  and  $j$  was defined to be the difference between the cross-correlation  $\chi_{ij}(t)$  integrated over a 200-ms window after time zero and the cross-correlation integrated over a 200-ms window preceding time zero (12) (Fig. 1B).

When pairs of cells displayed strong temporal ordering on the track, they tended in a statistically significant way to show a bias in the same direction during sleep that followed the track-running period, but not during sleep that preceded the track-running period. A particularly clear example is illustrated in Fig. 1C for one of the recording sessions. The central cluster of points in each panel represents pairs of cells having little or no overlap on the track; these clusters show a broad scatter of bias values during sleep both before and after track-running. The points whose horizontal coordinates are large, on the other hand, represent pairs of cells with place fields close to each other on the track; the bulk of these show a bias in the same direction during sleep that followed the track-running session.

The irregular distributions in Fig. 1C do not lend themselves very well to statistical analysis. We used two methods to quantify the relations. First, we calculated the correlation coefficient between the horizontal and vertical coordinates in each plot. If

there were no reproduction of temporal bias, then the expected correlation coefficient would be zero. Because correlation coefficients are hypersensitive to outliers, we supplemented this analysis by comparing the number of points in the upper right quadrant ( $N_{++}$ ) with the number of points in the lower right quadrant ( $N_{+-}$ ) for each plot. If there were no reproduction of bias, then these numbers would be expected to be equal. (Because the bias merely changes sign when the order of a pair of cells is reversed, the left quadrants contain no extra information.) Both of these methods are independent of the scale of the axes (13).

For all seven recording sessions, the correlation (Fig. 2A) during the "sleep after" period was greater than the correlation during the "sleep before" period. This consistency is statistically significant ( $P < 0.01$ ; one-tailed sign test). The mean correlation for the "sleep after" period was significantly larger than zero ( $P < 0.05$ ; Student's  $t$  test, one-tailed) and significantly larger than the correlation during the "sleep before" period ( $P < 0.01$ ; paired  $t$  test, one-tailed), which

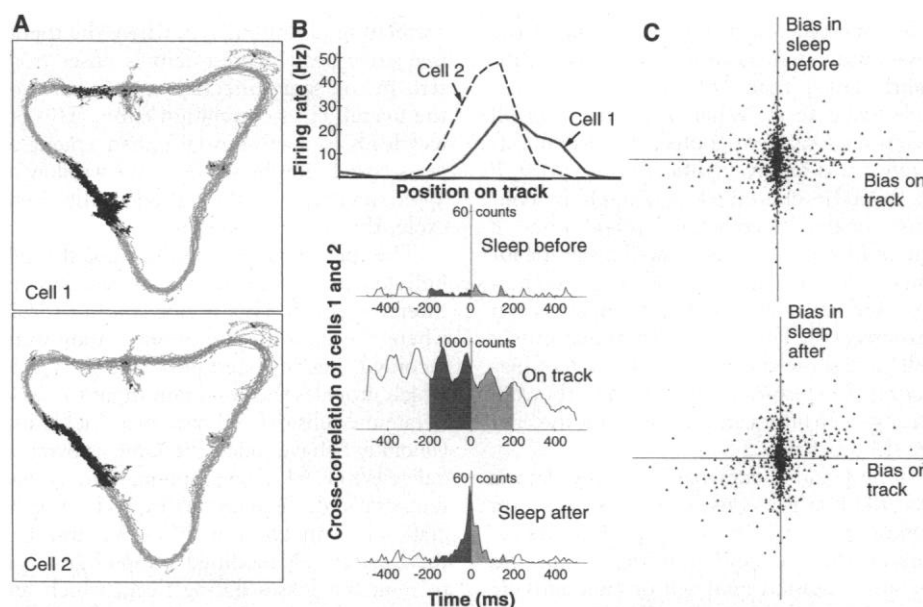
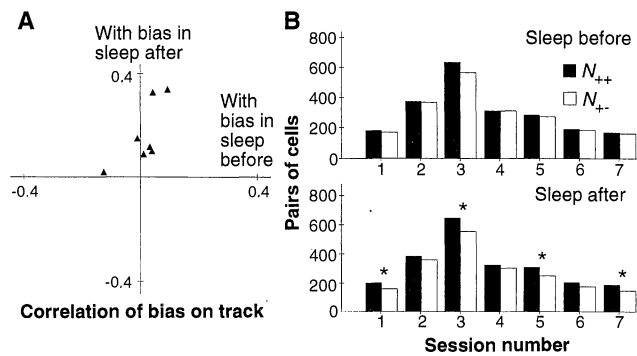


**Fig. 1.** Temporal bias of cross-correlations. **(A)** Spatial firing fields for a pair of simultaneously recorded CA1 pyramidal cells. The rat ran repeatedly counterclockwise along an elevated triangular track, stopping in the center of each side to consume a small food reward. The trajectory of the rat is shown in gray, and spikes fired by the cells are represented by small black dots. The place field of cell 1 is displaced slightly forward with respect to the place field of cell 2. **(B)** Firing rate and cross-correlation plots for the two cells in (A). (Top) Mean firing rate for each of the two cells, as a function of position on the track. The direction of motion is from left to right. (Bottom) Cross-correlation plots derived from data recorded while the rat slept 15 min before the track-running session (top), while the rat ran on the track (middle), and while the rat slept 15 min after the track-running session (bottom). The temporal bias of the pair of cells is measured by the difference in area of the light- and dark-shaded regions. Note the strong theta-frequency ( $\sim 8$  Hz) modulation of the cross-correlation during the track-running session. The cross-correlation plots for different pairs of cells during any of the three periods are highly variable; this example illustrates the overall pattern found in the data. The bin size for these plots is 10 ms. **(C)** Scatterplots of temporal bias while the rat ran on the track versus the bias during 15-min periods of sleep before and after the track-running session. Each point represents a single pair of CA1 pyramidal cells. This figure shows data from one of the seven recording sessions. Not all of the others showed such a salient effect, but the tendency was in all cases in the same direction. The scales for the axes differ, but the vertical-axis scale is the same for both plots.

**Fig. 2.** Relation of temporal bias on the track with bias before and after track running. **(A)** Scatterplot of correlation coefficients for the seven recording sessions. Each correlation coefficient is calculated from a plot of the type in Fig. 1C. The horizontal coordinate of each point represents the overall correlation, for all pairs of cells from the recording session, between the temporal bias during track running and the temporal bias during the 15 min of sleep before the track-running session. The vertical coordinate represents the correlation of the bias during track running and the bias during sleep after the track-running session. **(B)** Histogram plots of  $N_{+++}$  and  $N_{+-}$ , for each of the seven recording sessions, during periods of sleep before and after the track-running session. Asterisks mark sessions where  $N_{+++}$  is significantly greater than  $N_{+-}$  ( $P < 0.05$ ).



was not itself significantly different from zero. Thus, the bias during track running was more strongly correlated with the bias during sleep afterward than with the bias during sleep before.

For the "sleep after" period, all seven sessions yielded  $N_{+++} > N_{+-}$  (Fig. 2B); this consistency is statistically significant ( $P < 0.01$ ; one-tailed sign test). For four of the seven individual sessions,  $N_{+++}$  was significantly larger than  $N_{+-}$  ( $P < 0.05$ ; one-tailed sign test). When the data from all seven sessions were pooled, the overall difference was highly significant ( $Z = 4.79$ ,  $P < 0.00001$ ; one-tailed sign test). In contrast, for the "sleep before" period, none of the individual sessions showed a significant difference between  $N_{+++}$  and  $N_{+-}$ , and neither did the data pooled from all seven sessions (14). Thus, a significant majority of cell pairs showed the same direction of bias during the maze-running session as they did during sleep afterward; this was not the case for sleep before.

One possible explanation of the data is that the bias is a consequence of long-term potentiation (LTP) occurring while the rat runs on the track, either during the specific recording session analyzed or cumulatively during earlier experiences in the same environment (15). In order for this to occur, there would need to be some mechanism to make LTP sensitive to the order of cell firing. Several studies have indicated that potentiation of a synapse occurs preferentially when the presynaptic cell fires simultaneously with or before, but not after, the postsynaptic cell, within a window of about 40 ms (16). Thus, if two cells A and B are reciprocally connected and the pair AB shows a positive cross-correlation bias with a time window of 40 ms, then the connection from A to B is likely to be strengthened more than the connection from B to A. Evidence (17) indicates that when the place fields of two cells are overlapping but

offset such that the rat passes through their centers in rapid succession, then their cross-correlation histogram shows a theta-frequency peak offset from zero in the same direction. This offset is a consequence of the phase shifting of spike activity with respect to the theta cycle (17, 18) and is illustrated by the middle ("on track") cross-correlation plot in Fig. 1B, where the theta-frequency peak nearest zero is offset from zero in the same direction as the offset of the overall cross-correlation curve. This effect leads to a substantial enhancement of cross-correlation bias over a time window of approximately half the period of the theta cycle, that is, about 60 ms.

The proposed mechanism could only function in an area where cells are densely interconnected. This is not true for CA1, where the data for the present study were recorded, but it is certainly true for CA3, which provides the dominant input to CA1. Pyramidal cells in CA3 have place fields and generally behave much the same as pyramidal cells in CA1. The proposal, then, is that temporal order is recorded by LTP of associational connections within CA3, and that these selectively modified synapses give rise to temporal biases during sleep, which are then transferred to CA1 by way of the strong Schaffer collateral projection.

## REFERENCES AND NOTES

- W. B. Scoville and B. Milner, *J. Neurol. Neurosurg. Psychiatry* **20**, 11 (1957); for recent reviews, see (4); N. J. Cohen and H. Eichenbaum, *Memory, Amnesia, and the Hippocampal System* (MIT Press, Cambridge, MA, 1993).
- T. Lomo, *Acta Physiol. Scand.* **68**, 28 (1966); T. V. P. Bliss and T. Lomo, *J. Physiol.* **232**, 331 (1973); T. V. P. Bliss and A. R. Gardner-Medwin, *ibid.*, p. 357; R. M. Douglas and G. V. Goddard, *Brain Res.* **86**, 205 (1975); P. Andersen, S. H. Sundberg, O. Sveen, H. Wigström, *Nature* **266**, 736 (1977); B. L. McNaughton, R. M. Douglas, G. V. Goddard, *Brain Res.* **157**, 277 (1978); W. B. Levy and O. Steward, *ibid.* **175**, 233 (1979).
- D. Marr, *Philos. Trans. R. Soc. London* **262**, 23 (1971); T. J. Teyler and P. Discenna, *Behav. Neuro-*

*sci.* **100**, 147 (1986); A. Treves and E. T. Rolls, *Hippocampus* **4**, 374 (1994); J. L. McClelland, B. L. McNaughton, R. C. O'Reilly, *Psychol. Rev.* **102**, 419 (1995).

- L. R. Squire, *Psychol. Rev.* **99**, 195 (1992).
- G. Buzsáki, *Neuroscience* **31**, 551 (1989).
- J. O'Keefe and J. Dostrovsky, *Brain Res.* **34**, 171 (1971); D. S. Olton, M. Branch, P. J. Best, *Exp. Neurol.* **58**, 387 (1978); J. O'Keefe, *Prog. Neurobiol.* **13**, 419 (1979); B. L. McNaughton, C. A. Barnes, J. O'Keefe, *Exp. Brain Res.* **52**, 41 (1983); R. U. Muller, J. L. Kubie, J. B. Ranck Jr., *J. Neurosci.* **7**, 1935 (1987).
- C. Pavlides and J. Winson, *J. Neurosci.* **9**, 2907 (1989).
- M. A. Wilson and B. L. McNaughton, *Science* **265**, 676 (1994).
- G. Buzsáki, *Brain Res.* **398**, 242 (1986); A. Ylinen et al., *J. Neurosci.* **15**, 30 (1995).
- The CA1 cell body layer can be recognized by several criteria, including the presence of 100- to 300-Hz "ripples" in electroencephalograms recorded from the tetrodes, "sharp waves" in the electroencephalograms that reverse polarity about 50  $\mu$ m below the CA1 layer, and most importantly, the sudden appearance, at a depth about 2 mm below the dura, of large numbers of simultaneously recorded cells firing complex spikes [(9); J. O'Keefe, *Exp. Neurol.* **51**, 78 (1976); G. Buzsáki, Z. Horváth, R. Urioste, J. Hetke, K. Wise, *Science* **256**, 1025 (1992); S. S. Suzuki and G. K. Smith, *Electroencephalogr. Clin. Neurophysiol.* **69**, 541 (1987)]. The electrode arrays were implanted stereotaxically, under pentobarbital (Nembutal) anesthesia; all procedures were carried out in accordance with an institutionally approved animal care protocol. The CA1 layer was identified by standard electrophysiological criteria, and pyramidal cells (31 to 57 per recording session) were identified on the basis of action-potential wave forms and interspike interval histograms. To be classified as a pyramidal cell, a unit was required (i) to fire at least a small number of complex spike bursts during the recording session, (ii) to be recorded simultaneously with other cells firing complex spikes, (iii) to have a spike width (peak to valley) of at least 300  $\mu$ s; and (iv) to have an overall mean rate below 5 Hz during the recording session [J. B. Ranck Jr., *Exp. Neurol.* **41**, 461 (1973); S. Fox and J. B. Ranck Jr., *Exp. Brain Res.* **41**, 399 (1981); G. Buzsáki, L. S. Leung, C. H. Vanderwolf, *Brain Res. Rev.* **6**, 139 (1983)].
- The rats varied in familiarity with the task, some having been trained on the same track daily for only 6 days (but extensively trained on other, similar types of apparatus), others having performed the same task daily for several weeks, always at approximately the same time of day. Three of the rats were young adults, about 9 months old; the other three were elderly, 27 to 30 months old. One of the young rats was recorded from twice, on both triangle and rectangle, 2 weeks apart; the other five rats were recorded from once each. For each recording session, the rat was first placed on a small round platform near the track, and unit activity was monitored until a period of sleep lasting 30 min or more was recorded. Next, the rat was placed on the track, where it ran for food reward for 20 to 30 min. Finally, the rat was returned to the platform and recorded from for a further 30 to 60 min of sleep. During many of the sessions, the sleep periods were broken by brief intervals of drowsy wakefulness or arousal, during which place-specific firing of some units was seen on the platform, but this activity bore no apparent relation to the activity seen on the track. From each sleep session, a period of 15 min with minimal signs of arousal (that is, movement and theta activity in the EEG) was selected for analysis. It is difficult, with the information available, to distinguish clearly between SWS and a state of drowsy wakefulness, or between the physiology of these two states. The design of the study proceeded as follows. Initially, a data set with a large number of cells was chosen for preliminary analyses, working out the computational and statistical techniques. Next, we performed the same analyses on six more data sets, choosing this number because seven out of seven is significant at the 0.01 level in a sign test, given an a priori probability of 0.5.

The criteria were that there be a good number of cells, good behavior on the apparatus, and at least 15 min of good sleep both before and after the behavioral session. These were informal criteria, but the data sets were chosen before any analyses were performed on them. The data were taken from animals involved in a variety of experiments, including, for example, a study of the effects of aging on rat hippocampal activity. Every data set that was analyzed is presented in this report.

12. The value of the "cross-correlation" function  $\chi_{ij}(t)$ , as used here, was equal to the number of pairs of spikes, one from cell  $i$  and the other from cell  $j$ , that were separated by an interspike interval in the range  $(t, t + \Delta t)$ , where  $\Delta t$  is the bin size. The measure of temporal asymmetry used here is, however, independent of the bin size, so long as it is small. The measure of temporal asymmetry was

$$B_{ij} = \int_0^{200} \chi_{ij}(t) dt - \int_{-200}^0 \chi_{ij}(t) dt \quad (1)$$

$B_{ij}$  measures the difference between the number of events in which a spike from cell  $i$  was followed within 200 ms by a spike from cell  $j$  and the number of events in which a spike from cell  $j$  was followed within 200 ms by a spike from cell  $i$ , possibly with other spikes of either cell in between. Note that  $B_{ji} = -B_{ij}$ . This reversal of sign as a consequence of exchanging the cells makes the temporal bias measure quite different from a simple correlation measure of the type used by Wilson and McNaughton (8), which keeps the same value if the two cells are exchanged. To minimize the possibility of artifacts caused by shrinkage of spike amplitude when a cell is highly active, we used only pairs of cells recorded from different tetrodes in the analyses.

13. Our main concern in this study was to establish the reality of the phenomenon in as straightforward a way as possible. Therefore, we thought it preferable to avoid any manipulations of the data that were not absolutely necessary, such as rescaling or thresholding. It is likely that the relations reported here would be stronger if, for example, only pairs of cells with overlapping place fields were included.
14. As mentioned previously, we calculated the temporal bias in these analyses using a time window of  $\pm 200$  ms. We also experimented with time windows of 50, 100, 500, and 1000 ms. Significant effects could be seen for some of the recording sessions with time windows of 100 and 500 ms, but they appeared to be less consistent. We also experimented with different time windows for the sleep and track-running sessions, but again, time windows of 200 ms for both yielded the most consistent evidence for reproduction of temporal bias. During track running, a time window of 200 ms captures the relation of most pairs of cells with overlapping place fields but yields zero for most pairs whose fields are more widely separated; during sleep, a time window of 200 ms captures relations that occur within individual sharp waves but rarely encompasses two consecutive sharp waves. Buzsáki (5) suggested that behavioral sequences may be compressed into the time window of individual sharp waves, and Skaggs *et al.* (17) have shown evidence that sequences are compressed within individual theta cycles.
15. Long-term potentiation in the rat hippocampus is thought to have a duration of days to weeks [(2); C. A. Barnes, *J. Comp. Physiol. Psychol.* **93**, 74 (1979)]. Why, then, would temporal bias be reproduced preferentially during sleep after behavior in a familiar environment? One possibility is that the effects are the result of the early, decremental component of LTP, known as short-term potentiation, which has a time course of 5 to 40 min [R. Malenka, *Neuron* **6**, 53 (1991); A. Colino, Y.-Y. Huang, R. C. Malenka, *J. Neurosci.* **12**, 180 (1992)]. Another theoretical possibility, which remains to be explored, is that the observed pattern of temporal bias results from a combination of long-lasting temporally asymmetric LTP with a short-lasting postbehavioral enhancement of the activity level of individual units, as observed by Pavlides and Winson (7). However, no such enhancement in activity was observable in our data; this discrepancy may be because Pavlides and Winson obtained their results by confining each rat inside the place field of each cell for an extended period of time.

16. W. B. Levy and O. Steward, *Neuroscience* **8**, 791 (1983); B. Gustaffson and H. Wigström, *J. Neurosci.* **6**, 1575 (1986); J. Larson, D. Wong, G. Lynch, *Brain Res.* **368**, 347 (1986); J. Larson and G. Lynch, *ibid.* **489**, 49 (1989); Y. J. Greenstein, C. Pavlides, J. Winson, *ibid.* **438**, 331 (1988); D. M. Diamond, T. V. Dunwiddie, G. M. Rose, *J. Neurosci.* **8**, 4079 (1988); C. Pavlides, Y. J. Greenstein, M. Grudman, J. Winson, *Brain Res.* **439**, 383 (1988); T. H. Brown, A. M. Zador, Z. F. Mainen, B. J. Claiborne, in *Long-Term Potentiation: A Debate of Current Issues*, M. Baudry and J. L. Davis, Eds. (MIT Press, Cambridge, MA, 1991), p. 357.

17. W. E. Skaggs, B. L. McNaughton, M. A. Wilson, C. A. Barnes, *Hippocampus*, in press.
18. J. O'Keefe and M. L. Recce, *ibid.* **3**, 317 (1993).
19. Supported by National Institutes of Health grant AG12609, National Institute of Mental Health grant MH46823, and the McDonnell-Pew Foundation. We thank M. A. Wilson for contributing in numerous ways to the analysis and C. A. Barnes, K. Moore, M. Suster, R. D'Monte, K. Weaver, C. Duffield, and K. Stengel for assistance with data acquisition and analysis.

6 November 1995; accepted 7 February 1996

## An RNA Polymerase II Elongation Factor Encoded by the Human *ELL* Gene

Ali Shilatifard, William S. Lane, Kenneth W. Jackson, Ronald C. Conaway, Joan W. Conaway\*

The human *ELL* gene on chromosome 19 undergoes frequent translocations with the *trithorax*-like *MLL* gene on chromosome 11 in acute myeloid leukemias. Here, *ELL* was shown to encode a previously uncharacterized elongation factor that can increase the catalytic rate of RNA polymerase II transcription by suppressing transient pausing by polymerase at multiple sites along the DNA. Functionally, *ELL* resembles Elongin (SII), a transcription elongation factor regulated by the product of the von Hippel-Lindau (*VHL*) tumor suppressor gene. The discovery of a second elongation factor implicated in oncogenesis provides further support for a close connection between the regulation of transcription elongation and cell growth.

The identification of genes at breakpoints of frequently occurring chromosomal translocations has led to the discovery of cellular proteins that are involved in oncogenesis. The fact that many of these proteins are transcription factors illustrates the critical role of transcriptional deregulation in human cancer (1, 2). One form of acute myeloid leukemia results from a t(11;19)(q23;p13.1) translocation between the *ELL* gene (also called *MEN*) on chromosome 19 and the *MLL* gene (also called *Htrx*, *ALL-1*, and *HRX*) on chromosome 11 (3). The predicted open reading frame (ORF) of the human *ELL* gene provides few clues to its role in either normal cell growth or leukemogenesis; the *ELL* gene encodes a basic, 621-amino acid protein that is ubiquitously expressed and highly conserved throughout evolution but exhibits no obvious homology to known proteins (3). The *MLL* gene encodes a 3968-amino acid protein; the NH<sub>2</sub>-terminal regions of *MLL* are similar to A-T hook DNA-binding and methyltransferase-like domains, and the COOH-terminal region of *MLL* is similar to that encoded by the *Drosophila* gene *trithorax* with a transcrip-

tional activation domain downstream of several contiguous zinc fingers (4, 5). The putative oncogene generated by the t(11;19) translocation encodes an NH<sub>2</sub>-*MLL*-*ELL*-COOH fusion protein that contains nearly the entire *ELL* ORF and the NH<sub>2</sub>-terminal 1300 amino acids of *MLL*, including its A-T hook and methyltransferase-like domains but lacking its COOH-terminal transcriptional activation domain and zinc fingers (3).

Recently, we purified an RNA polymerase II transcription factor from rat liver nuclear extracts by means of the procedure outlined in Fig. 1A (6). During purification, this factor was assayed by its ability to stimulate the rate of accumulation of 135-nucleotide (nt) transcripts synthesized by RNA polymerase II on the T-less cassette of the oligo(dC)-tailed template pCpGR220 S/P/X (7, 8). Analysis by SDS-polyacrylamide gel electrophoresis (PAGE) of fractions from the final PLRP-S reversed-phase high-performance liquid chromatography (rpHPLC) column revealed that transcriptional activity copurified with a single ~80-kD polypeptide (p80) (Fig. 1B), which stimulates transcription by RNA polymerase II in a dose-dependent manner (Fig. 1C). Results of pulse-chase experiments indicated that the factor is capable of stimulating the rate of elongation of promoter-specific transcripts synthesized by RNA polymerase II. Transcription was initiated at the adenovirus 2 major late (AdML) promoter by addition of adenosine triphosphate (ATP), guanosine triphosphate

A. Shilatifard, R. C. Conaway, J. W. Conaway, Program in Molecular and Cell Biology, Oklahoma Medical Research Foundation, Oklahoma City, OK 73104, USA.

W. S. Lane, Harvard Microchemistry Facility, Harvard University, 16 Divinity Avenue, Cambridge, MA 02138, USA.

K. W. Jackson, William K. Warren Medical Research Institute, University of Oklahoma Health Sciences Center, Oklahoma City, OK 73190, USA.

\*To whom correspondence should be addressed.